Copy 199

RM A9F20

CONFIDENTIAL

NACA RM A9F20

NACA

RESEARCH MEMORANDUM

AN EXPERIMENTAL INVESTIGATION AT LARGE SCALE OF SINGLE AND TWIN NACA SUBMERGED SIDE INTAKES AT SEVERAL ANGLES OF SIDESLIP

By Norman J. Martin and Curt A. Holzhauser

Ames Aeronautical Laboratory
Moffett Field, Calif.

CLASSIFICATION CHANGED TO

UNCLASSIFIED DATE 8-18-54

AUTHORITY J.W.CROWLEY

CHANGE # 2443 W.H.L.

CLASSIFIED DOCUMENT

This document contains classified information affecting the National Defense of the United States within the meaning of the Espionage Act, USC 50:31 and 32. Its transmission or the revelation of its contents in any manner to an unauthorized person is prohibited by law. Information so classified may be imparted only to persons in the military and naval services of the United States, appropriate civilian officers and employees of the Federal Government who have a legitimate interest therein, and to United States citizens of known loyalty and discretion who of necessity must be informed thereof.

NATIONAL ADVISORY COMMITTEE FOR AERONAUTICS

WASHINGTON
August 1, 1949

CONFIDENTIAL

NATIONAL ADVISORY COMMITTEE FOR AERONAUTICS

RESEARCH MEMORANDUM

AN EXPERIMENTAL INVESTIGATION AT LARGE SCALE OF SINGLE AND TWIN NACA SUBMERGED SIDE INTAKES AT SEVERAL ANGLES OF SIDESLIP

By Norman J. Martin and Curt A. Holzhauser

SUMMARY

Results of an experimental investigation to determine the pressure-recovery and mass-flow characteristics of single and twin NACA submerged intakes on the sides of a fuselage at various angles of sideslip are presented. Tests were conducted with the single and twin submerged intakes installed on a full-scale model of a fighter-type airplane.

The twin-intake air-induction system had unstable air-flow characteristics when operating at mass-flow ratios lower than 0.40.

The single and twin NACA submerged-intake installations had similar pressure-recovery characteristics at mass-flow ratios for stable flow with the model at 0° sideslip. For both single and twin submerged-intake installations, increasing the angle of sideslip increased the pressure recovery of the intake toward which sideslip was being made and decreased the pressure recovery of the intake on the side opposite the direction of sideslip. The effect of sideslip on pressure recovery was greater for a single than for a twin submerged-intake installation. However, in the usual flight operating range the variation with sideslip of the pressure recovery of submerged side intakes was small.

INTRODUCTION

An experimental investigation at large scale of an NACA submerged intake indicated the same favorable characteristics for the intake that had been noted at small scale. (See reference 1.) The maximum values of ram-recovery ratio were high (0.92 for the full-scale intake without deflectors) and the variation of ram-recovery ratio with angle of attack was small. This information was obtained from tests of a single intake on the side of a fuselage at 0° sideslip. Previous small-scale tests (reference 2) have also indicated that under certain conditions an unstable type of flow may be experienced in air-induction systems in which the air flow of two intakes join in a common duct.

Since an airplane may utilize an air-induction system employing either one intake or twin intakes and will operate at angles of sideslip other than 0°, it is the purpose of this investigation to determine at large scale the pressure-recovery and air-flow characteristics of both single and twin NACA submerged side intakes at several angles of sideslip.

NOTATION

Symbols

A duct area, square feet

H total pressure, pounds per square foot

p static pressure, pounds per square foot

q dynamic pressure, pounds per square foot

V velocity of the air stream, feet per second

α geometric model angle of attack referred to fuselage center line (nose up is positive direction), degrees

β model angle of sideslip, angle between fuselage center line and flight path (nose to left is positive direction), degrees

ρ mass density of the air, slugs per cubic foot

Subscripts

o free stream

1 duct station 1

2 duct station 2

l local

ind individual

sys system

Parameters

$\frac{m_1}{m_o}$ the ratio of the mass flow in the duct to the mass flow of air in the free stream passing through an area equal to the entrance area of the intake $\left(\frac{\rho_1 A_1 V_1}{\rho_o A_1 V_o}\right)$

$\frac{\Delta H}{H_o}$ the ratio of the total pressure deviation at duct station 2 to the free-stream total pressure $\left(\frac{H_l - H_{sys}}{H_o}\right)$

$\frac{V_l - V_{sys}}{V_{sys}}$ the ratio of the velocity deviation at duct station 2 to the system velocity at duct station 2

$\frac{H - p_o}{H_o - p_o}$ ram-recovery ratio

DESCRIPTION OF MODEL AND APPARATUS

The full-scale model of a jet-propelled fighter-type airplane with twin NACA submerged intakes installed is shown mounted in the Ames 40- by 80-foot wind tunnel in figure 1. Tests of a single submerged intake were made of the right intake only with the left intake completely sealed. The ramp configuration used in all tests was the 7° standard curved-diverging-ramp intake described in reference 1.

A schematic drawing showing the general arrangement, instrumentation, and principal dimensions of the model is presented in figure 2. Coordinates of the fuselage nose, lip, and deflectors are given in reference 1. Shown in figure 3 are the shape and the dimensions of the duct at the stations where pressure measurements were made. The entrance station (duct station 1) was located 6.5 inches aft of the submerged-lip leading edge. The measuring station after partial diffusion (duct station 2) was located 62.5 inches aft of the entrance station and 22 inches forward of the station where the two ducts merged. The ratio of the duct area at duct station 2 to the duct area at duct station 1 was 1.52.

Each duct was instrumented with two rakes. One rake, consisting of 138 equally spaced total-pressure tubes and 37 static-pressure tubes, was installed at the entrance station, and another rake, having 66 equally spaced total-pressure tubes and 34 static-pressure tubes, was installed at duct station 2.

The mass-flow rate through the air-induction system was regulated by means of controllable louvers and a variable-speed axial-flow fan. A rake comprised of 20 equally spaced total-pressure tubes and 8 static-pressure tubes was used at the air outlet (fuselage station 455) to measure the quantity of air flow through the system. The quantity of air flow through each individual duct was determined from measurements provided by each rake at duct station 2.

The total-pressure tubes of each rake were connected to an integrating, water-in-glass manometer which provided an arithmetic-mean

reading of the total pressure. Individual tube readings of all manometers were recorded photographically.

TESTS

The pressure-recovery and the mass-flow characteristics of the single-intake and the twin-intake installations were determined for the following conditions:

1. Without deflectors – a mass-flow-ratio range of 0.1 to 1.4, a sideslip range of -12° to 12°, and an angle-of-attack range of -2° to 5° (C_L range of 0 to 0.59)

2. With deflectors – a mass-flow-ratio range of 0.1 to 1.4 at -6°, 0°, and 6° angles of sideslip and -2° angle of attack

The tunnel airspeed was maintained at approximately 160 miles per hour except at $\pm 12^{\circ}$ sideslip in which case the tunnel airspeed was reduced to approximately 120 miles per hour.

The entrance pressure-recovery characteristics of the twin submerged-intake installation were measured for the right intake only. When these entrance pressure measurements were being made, a similar rake was installed in the left intake to maintain a symmetrical configuration. The pressure recovery at duct station 2 was measured for both intakes simultaneously. When pressure-recovery measurements at station 2 were being made, the rakes at the entrance stations were removed.

RESULTS AND DISCUSSION

Twin Submerged Side Intakes on Model at 0° Sideslip

The pressure-recovery and flow characteristics of a twin submerged-intake installation will depend to a large extent upon the symmetry of the twin submerged-intake model tested. The symmetry of the present model was determined by testing each intake as a separate installation and comparing the pressure-recovery characteristics. As shown in figure 4, the maximum difference between the entrance ram-recovery ratios of the left and right intakes was 0.015 for the range of mass-flow ratios of the tests.

The variation with system mass-flow ratio of the ram-recovery ratio measured after partial diffusion (duct station 2) is shown in figure 5. The distribution of mass flow between the two intakes of the twin-intake air-induction system is given in figure 6. As may be observed in figure 5, the variation with system mass-flow ratio of ram-recovery ratio of each intake of the twin-intake installation was similar to that of the single-intake installation at system mass-flow ratios

of 0.40 and higher. At system mass-flow ratios lower than 0.40 the air flow in the twin-intake air-induction system had unstable characteristics. At system mass-flow ratios between 0.30 and 0.40, the pressure recovery and mass flow of one intake differed from that of the other intake and differed from that of a single-intake air-induction system. At system mass-flow ratios lower than 0.30, the air flow in one duct reversed direction of flow with a consequent increase of mass-flow ratio through the other duct. (See fig. 6.) The reversal of flow occurred in either the left or the right duct. The flow reversed in the duct which had the lower pressure recovery at the time the system mass-flow ratio was reduced to a value lower than 0.30. Once reversal of flow existed in one duct, that duct continued to have reversed flow until the system mass-flow ratio was increased to a value greater than 0.30.

As shown in figure 7, the deflectors had the same effect on the ram-pressure-recovery characteristics as had been determined in reference 1; the mass-flow ratio for maximum ram-recovery ratio after partial diffusion was increased by 0.25 (from 0.45 to 0.70). The addition of deflectors also resulted in a greater range of unstable flow; the minimum mass-flow ratio for stable flow was 0.50 compared to 0.40 without deflectors.

Single Submerged Side Intake on Model at Various Angles of Sideslip

The effect of sideslip on entrance ram-recovery ratio and ram-recovery ratio after partial diffusion is shown in figures 8 and 9, respectively. Figures 8 and 9 are derived from faired curves of actual test points. As shown in figures 8 and 9, the effect of sideslip on pressure recovery of the right single-intake installation is to increase the ram-recovery ratio with positive sideslip and to decrease the ram-recovery ratio with negative sideslip. The reduction of ram-recovery ratio at duct station 2 caused by 12° negative sideslip was 0.14 at mass-flow ratios of 0.7 and 1.1; the increase of ram-recovery ratio caused by 12° positive sideslip was 0.02 at a mass-flow ratio of 0.7 and was 0.05 at a mass-flow ratio of 1.1. However, the change of ram-recovery ratio was less than 0.02 in the probable range of sideslip angle ($\pm 1\text{-}1/2^{\circ}$) for high-speed flight. Thus, the effect of sideslip on the ram-recovery ratio of an NACA submerged side intake is of small significance. This would not be the case if the intake were considered located 90° to its present position so that the present angle of sideslip would be considered angle of attack.

The effect of angle of attack on ram-recovery ratio of a single intake on the model at various angles of sideslip was small and was similar to that shown in reference 1 for 0° sideslip.

Twin Submerged Side Intakes on Model at Various Angles of Sideslip

The effect of sideslip on entrance ram-recovery ratio and ram-recovery ratio after partial diffusion for a twin submerged-intake installation is shown in figures 10 and 11. Both of these figures are derived from faired curves of actual test data obtained at mass-flow ratios for stable flow. Entrance ram-recovery ratio was obtained for only the right intake.

Although the trend of the variation with sideslip of the ram-recovery ratio for the right intake of the twin-intake installation was, in general, similar to that of the single-intake installation (cf., figs. 8 and 10 and figs. 9 and 11(b)), the magnitude of the variation differed. The curves of figures 9 and 11(b) are compared in figure 12 to illustrate the difference. This difference resulted from a change in the distribution of the air flow between the intakes of the twin-intake installation; there was an increase of air flow through the inlet toward which sideslip was being made and a decrease of air flow through the opposite inlet. (See fig. 13.) As shown in figure 5, in the stable flow range the effect of increasing the mass flow through one intake was to decrease the ram-pressure recovery of that intake; and, conversely, the effect of reducing the air flow through the other intake was to increase the ram-pressure recovery of that intake. Thus, the change of mass-flow ratio of each intake tended to counteract the direct effect of sideslip on the pressure recovery (i.e., that effect of increasing the pressure recovery of the intake toward which sideslip was being made and decreasing the pressure recovery of the other intake).

As shown by a comparison of figures 9 and 11(c), the effect of sideslip on the system ram-recovery ratio at duct station 2 for the twin-intake installation was less than that for the single-intake installation. The loss of system ram-recovery ratio for the twin-intake system caused by 12° sideslip was 0.03 at a system mass-flow ratio of 0.7 and was 0.04 at a system mass-flow ratio of 1.3.

As may be observed in comparing figures 6 and 13, the effect of sideslip on the mass-flow ratio for unstable or reversed flow was small.

Total-Pressure and Velocity Distributions

The distributions of the total-pressure and velocity parameters after partial diffusion for a twin submerged-intake installation at 0°, 6°, and 12° sideslip are shown in figures 14 and 15. Since these distributions are for station 2 and not for the compressor inlet of a typical axial-flow jet engine, they are not truly representative of the total-pressure and velocity parameter distributions to be expected at the compressor of an axial-flow jet engine. These distributions are indicative only of the total-pressure and velocity parameter distributions

to be expected in vaneless straight diffusers used in combination with submerged intakes at the test speeds. The total-pressure and velocity parameter distributions are not known for a station at which the two flows have joined.

As shown in figure 14, the maximum total-pressure deviation tended to increase with increasing mass-flow ratio and with increasing angle of sideslip at system mass-flow ratios above 0.45. The maximum values of the ratio of velocity deviation to the system velocity, at system mass-flow ratios where stable flow existed, tended to remain approximately constant. When reversed flow occurred, the ratio of velocity deviation to the system velocity was high.

CONCLUSIONS

As the result of the experimental investigation at large scale of the pressure-recovery and air-flow characteristics of NACA submerged intakes, it was concluded that:

1. Twin air-induction systems with flows that join in a common duct are subject to an unstable type of air flow in which the pressure recovery and mass flow of one duct may become different from that of the other.

2. Each intake of the twin-intake air-induction system had pressure-recovery characteristics which were similar to those of a single-intake system when compared at the individual mass-flow ratio of the intake.

3. The effect of sideslip on the pressure recovery of the submerged side intakes was small in the usual flight operating range.

4. The variation with sideslip of the ram-recovery ratio of a twin-intake system was less than that for the single-intake system.

Ames Aeronautical Laboratory,
National Advisory Committee for Aeronautics,
Moffett Field, Calif., June 10, 1949.

REFERENCES

1. Martin, Norman J., and Holzhauser, Curt A.: An Experimental Investigation at Large Scale of Several Configurations of an NACA Submerged Air Intake. NACA RM A8F21, 1948.

2. Mossman, Emmet A., and Gault, Donald E.: Development of NACA Submerged Inlets and a Comparison with Wing Leading-Edge Inlets for a 1/4-Scale Model of a Fighter Airplane. NACA RM A7A31, 1947.

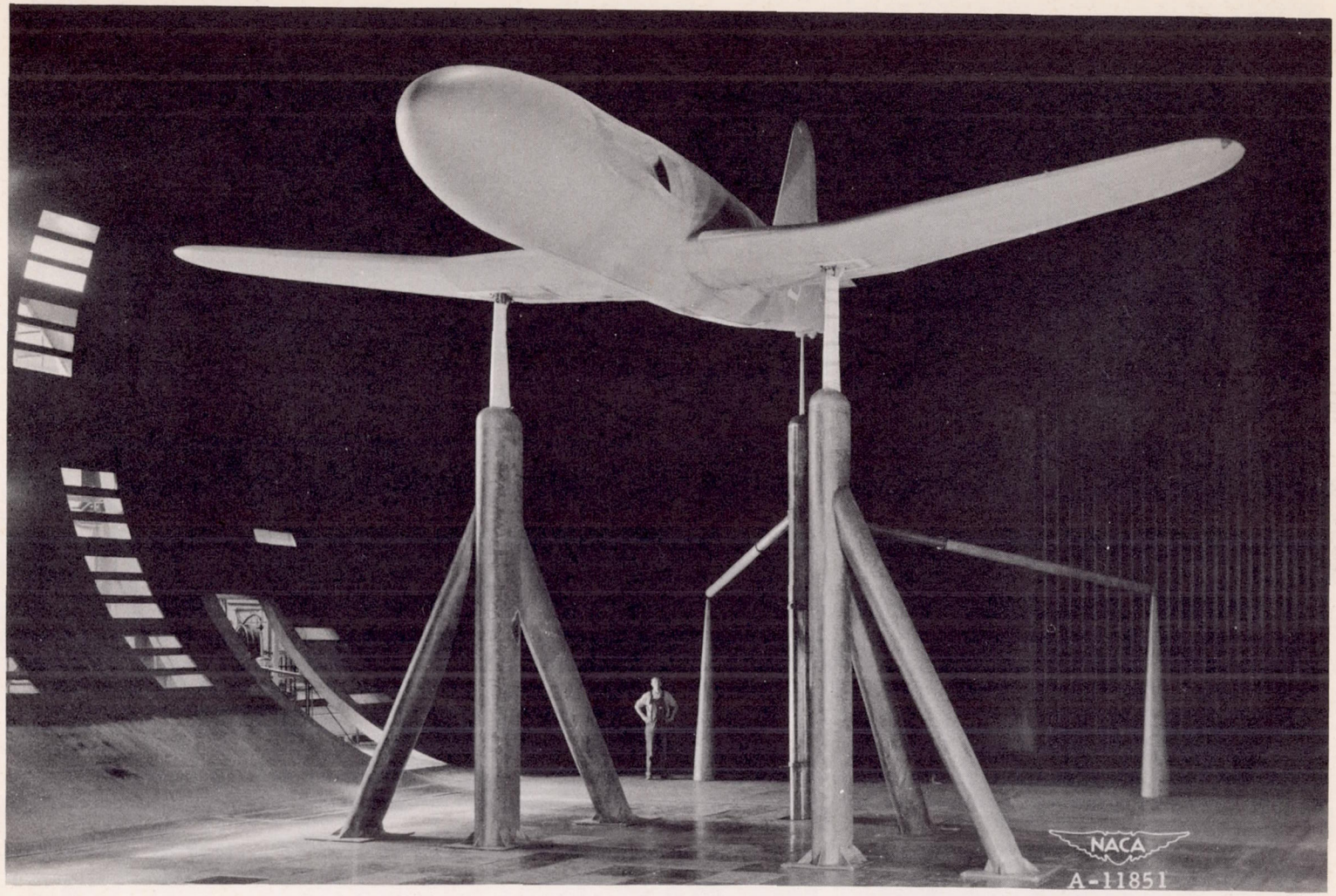

Figure 1.- The full-scale model with twin NACA submerged air intakes and deflectors installed.

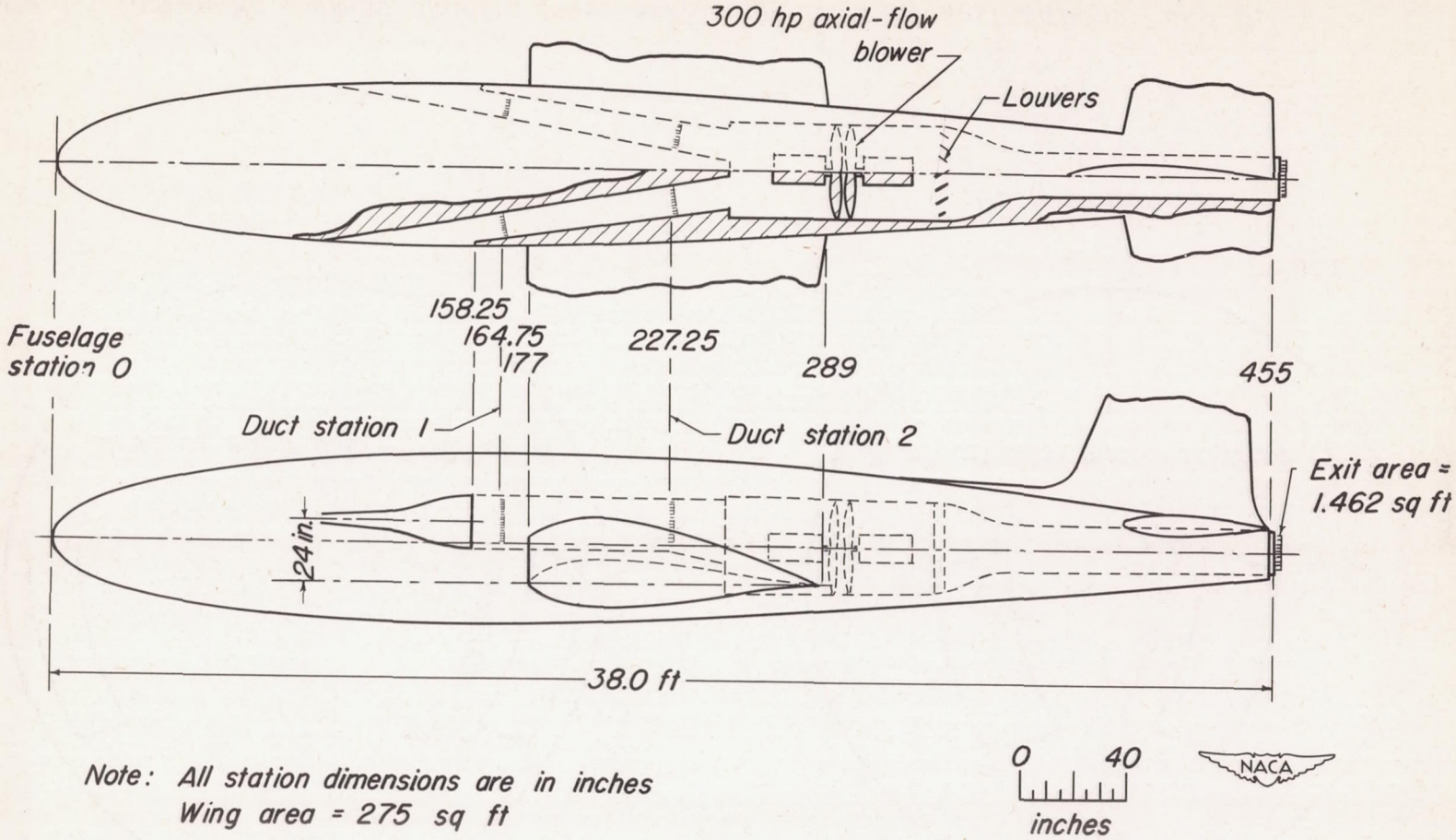

Note: All station dimensions are in inches
Wing area = 275 sq ft

Figure 2.- Schematic drawing showing arrangement of the full-scale model with twin NACA submerged side air intakes installed.

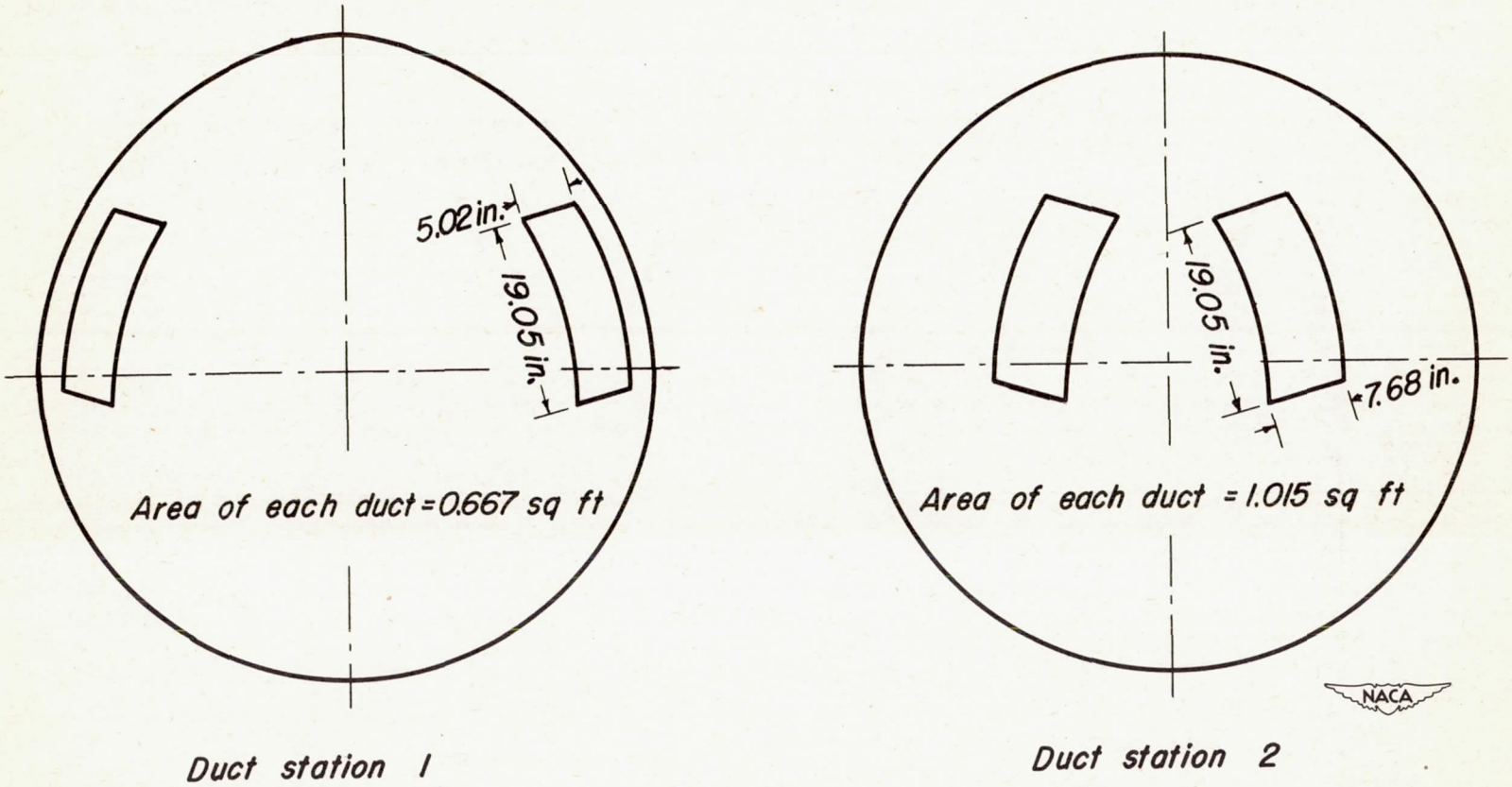

Figure 3.– Schematic drawing showing cross section of ducts at duct stations 1 and 2.

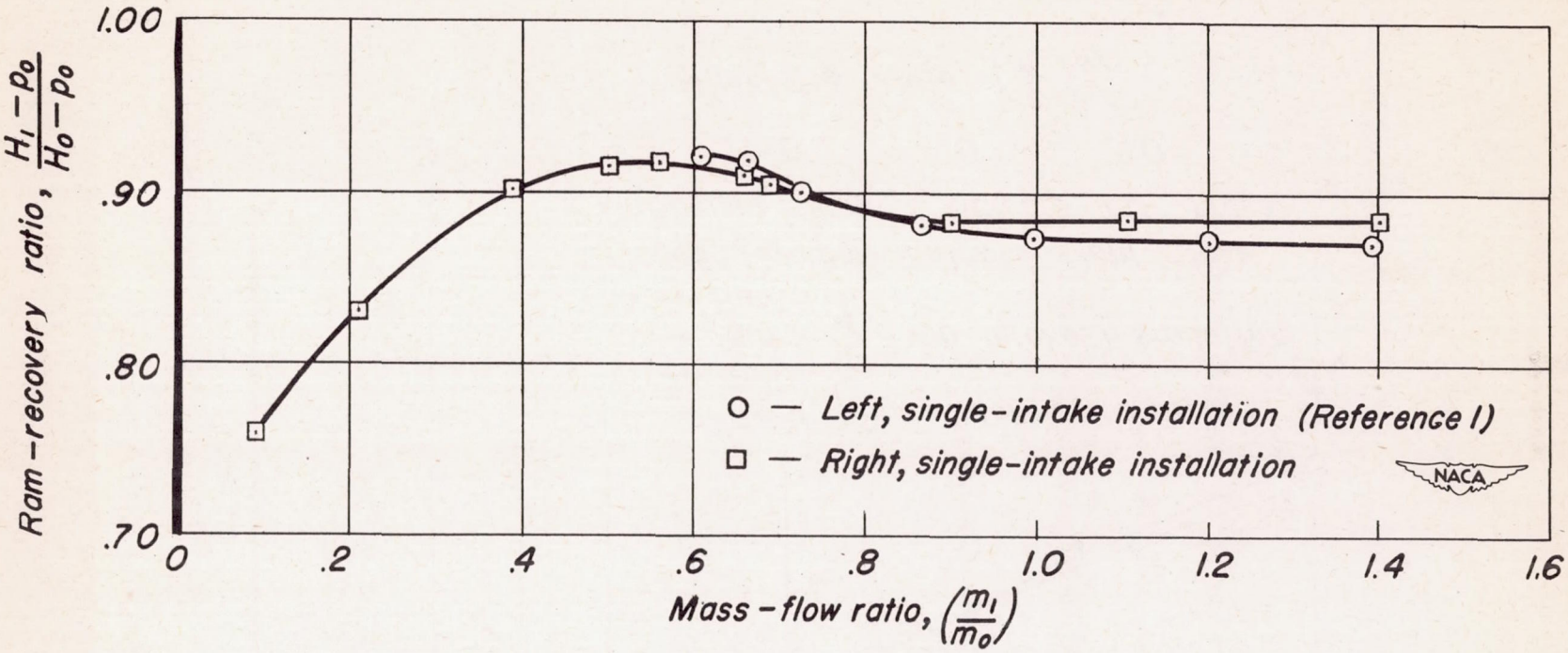

Figure 4.- Entrance pressure-recovery characteristics of a left and a right, single-intake installation; $\alpha = -2°$, $\beta = 0°$.

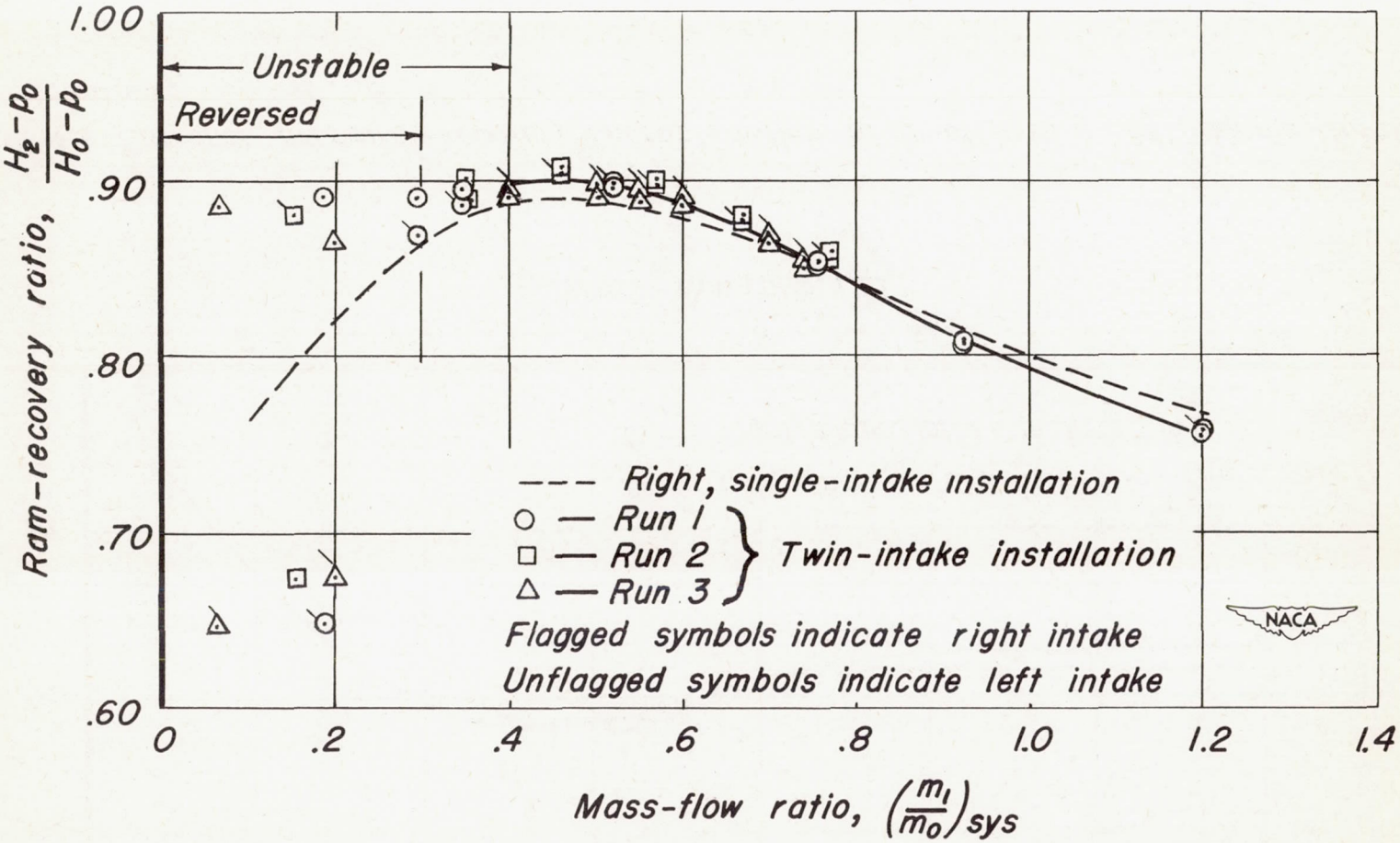

Figure 5.– The effect of mass-flow ratio on the pressure recovery, measured after partial diffusion, of a single- and a twin-intake installation; $\alpha = -2°$, $\beta = 0°$.

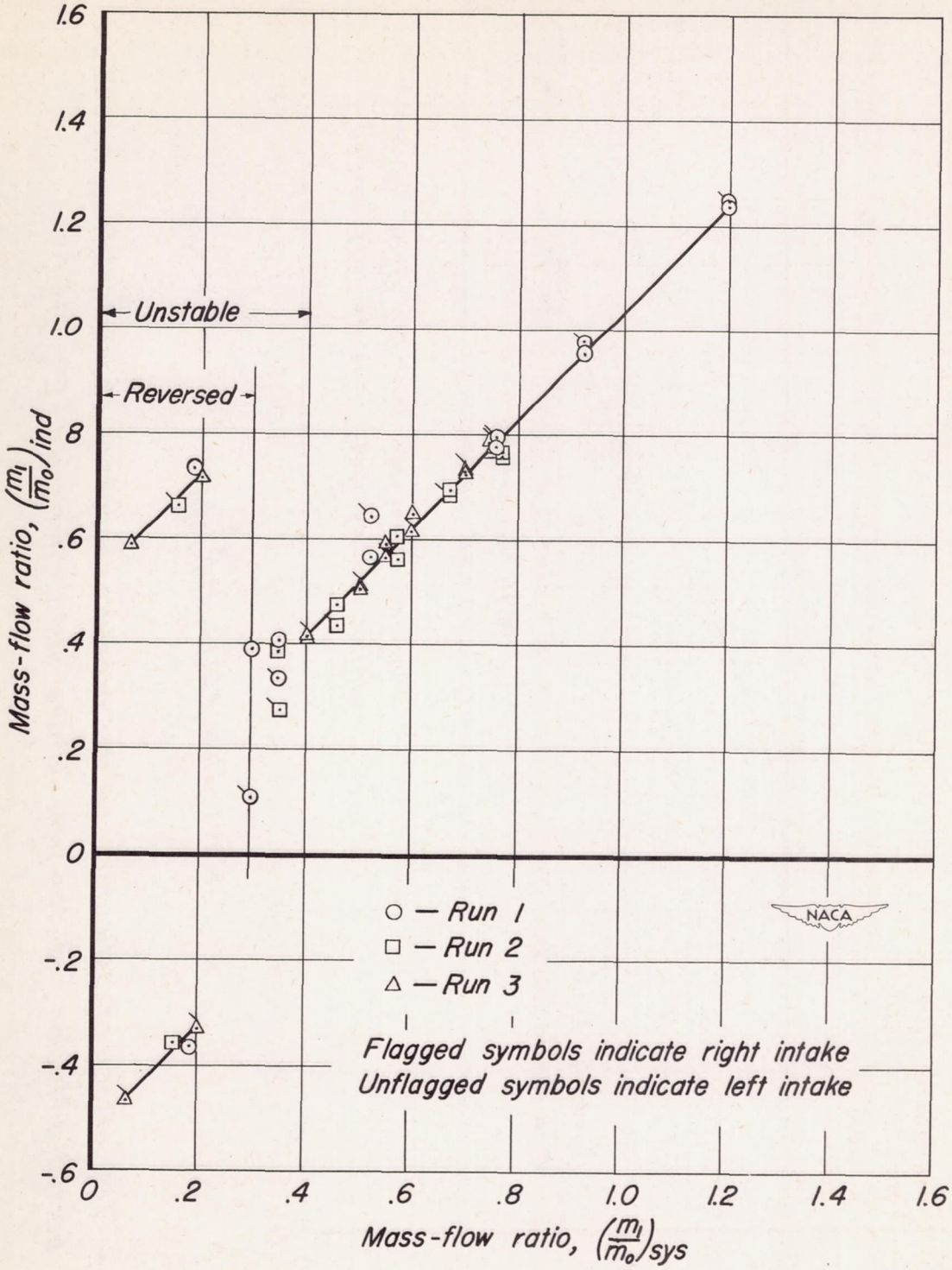

Figure 6.- The variation of mass-flow ratio of each intake with system mass-flow ratio of a twin-intake installation; $\alpha = -2°$, $\beta = 0°$.

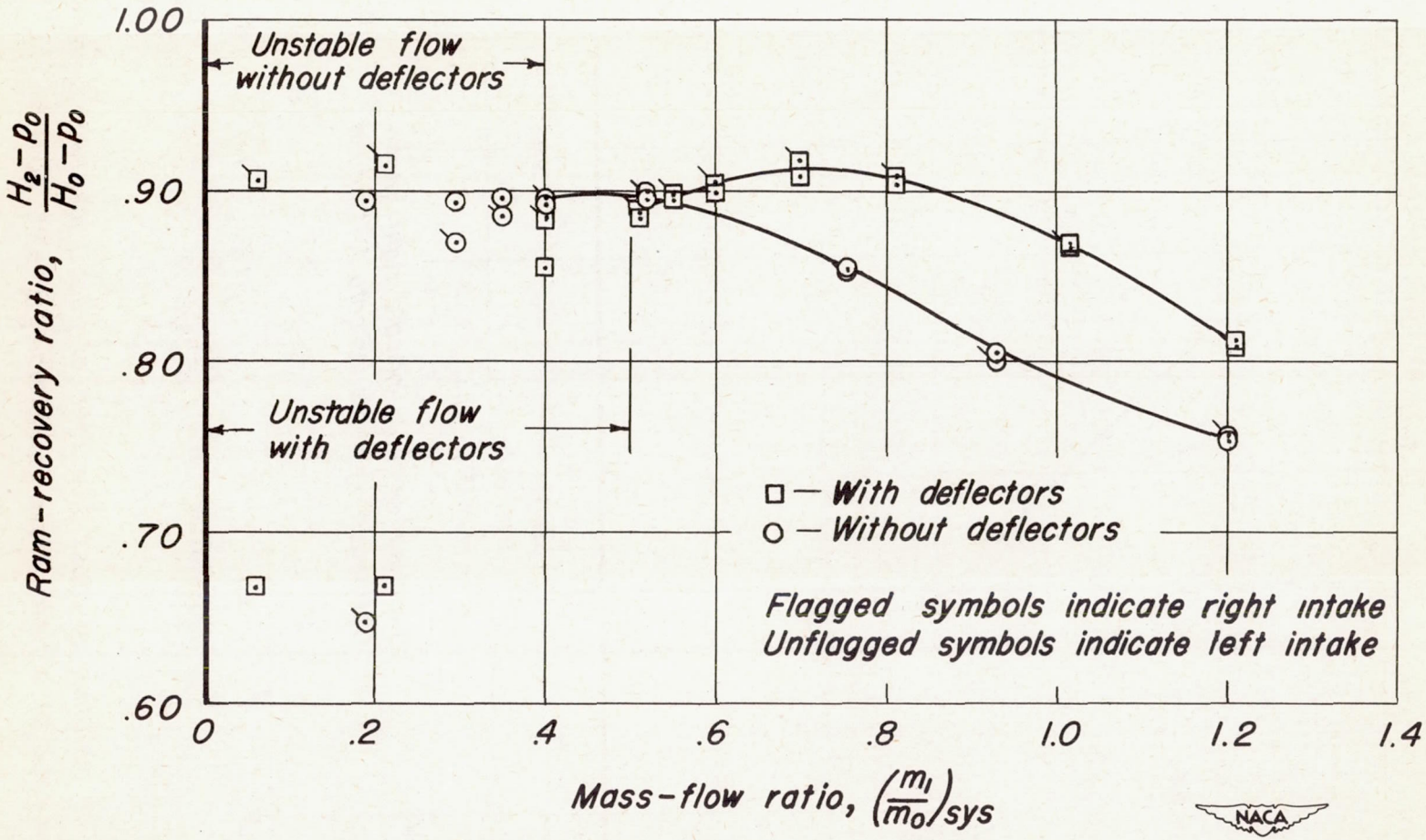

Figure 7.— The effect of deflectors on the pressure-recovery characteristics, measured after partial diffusion, of the twin-intake installation; $\alpha = -2°$, $\beta = 0°$.

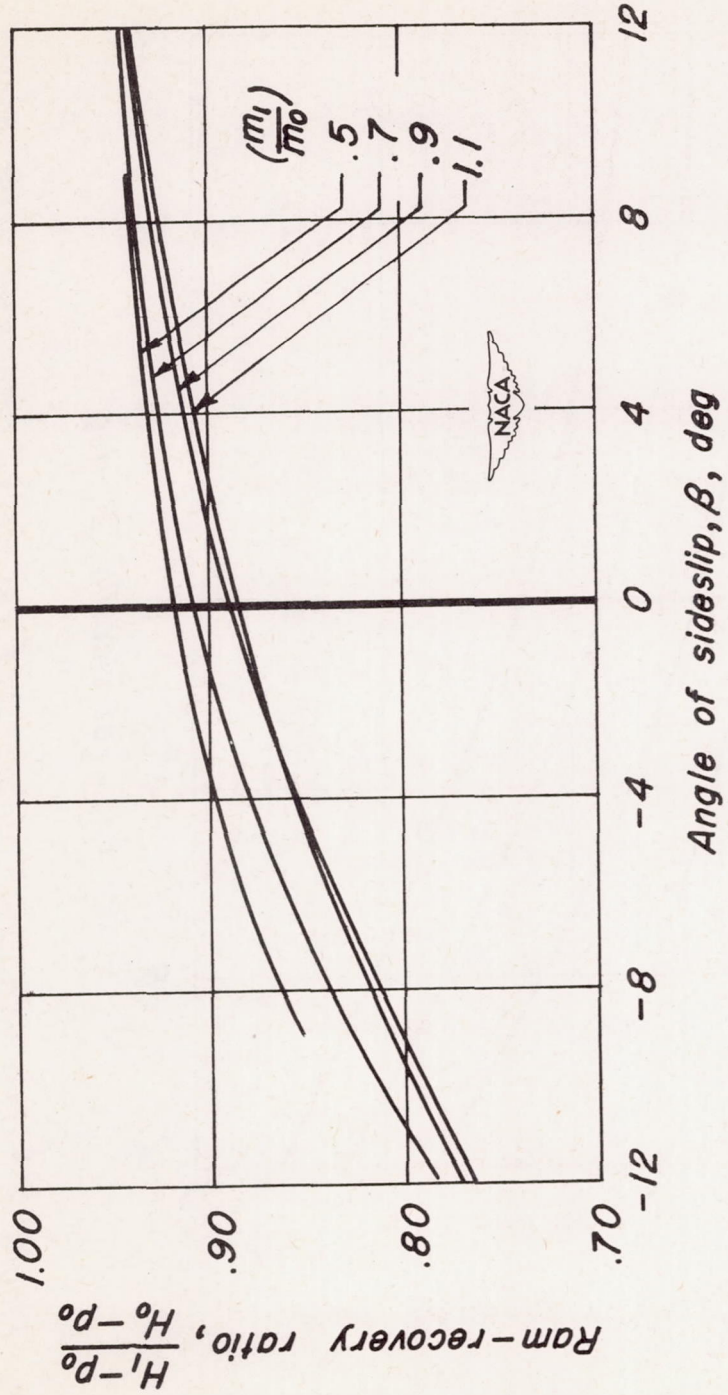

Figure 8.- The variation of entrance pressure recovery with sideslip of the right, single-intake installation; $\alpha = -2°$.

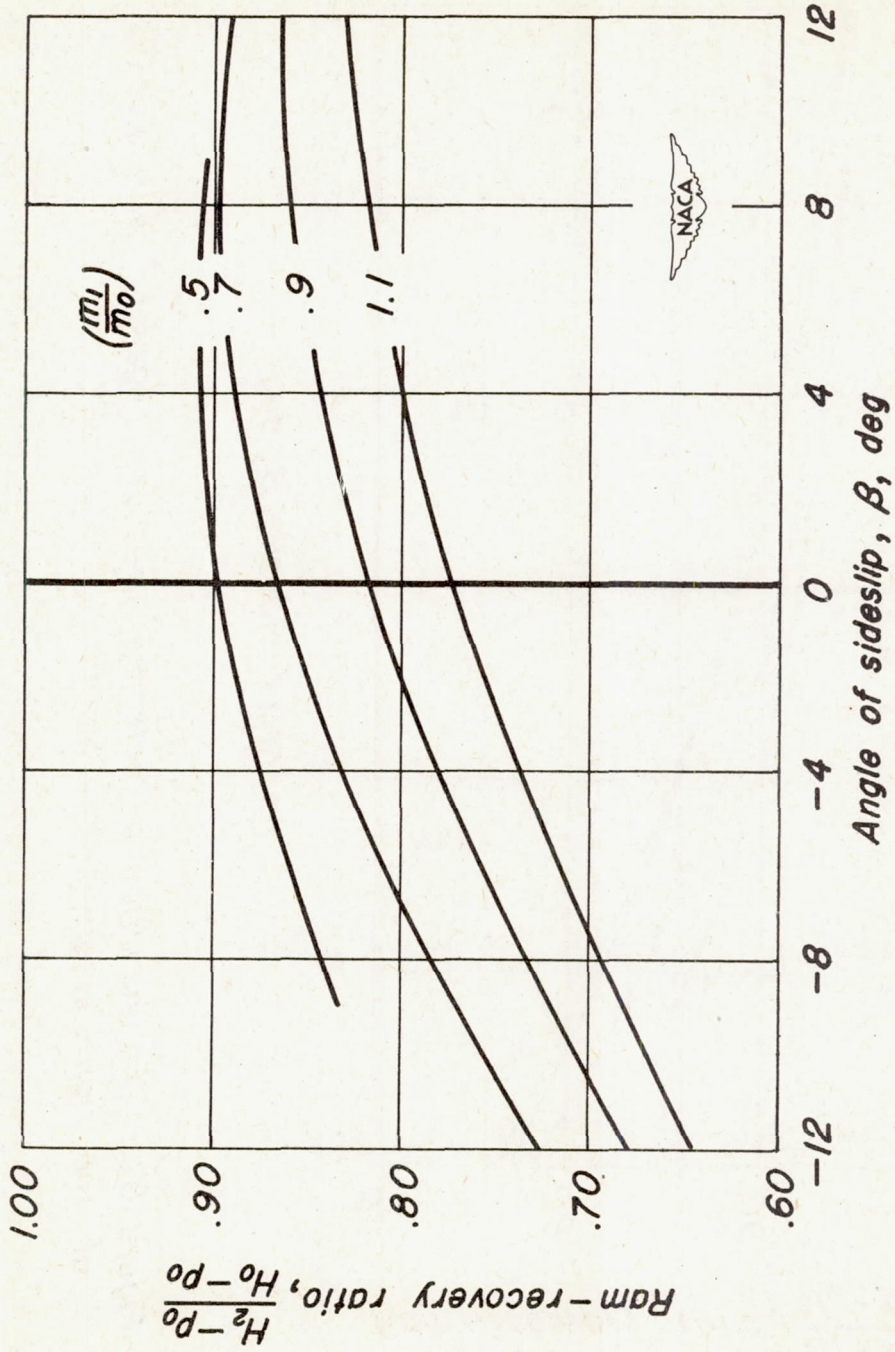

Figure 9.— The variation of pressure recovery, measured after partial diffusion, with sideslip of the right, single-intake installation; $\alpha = -2°$.

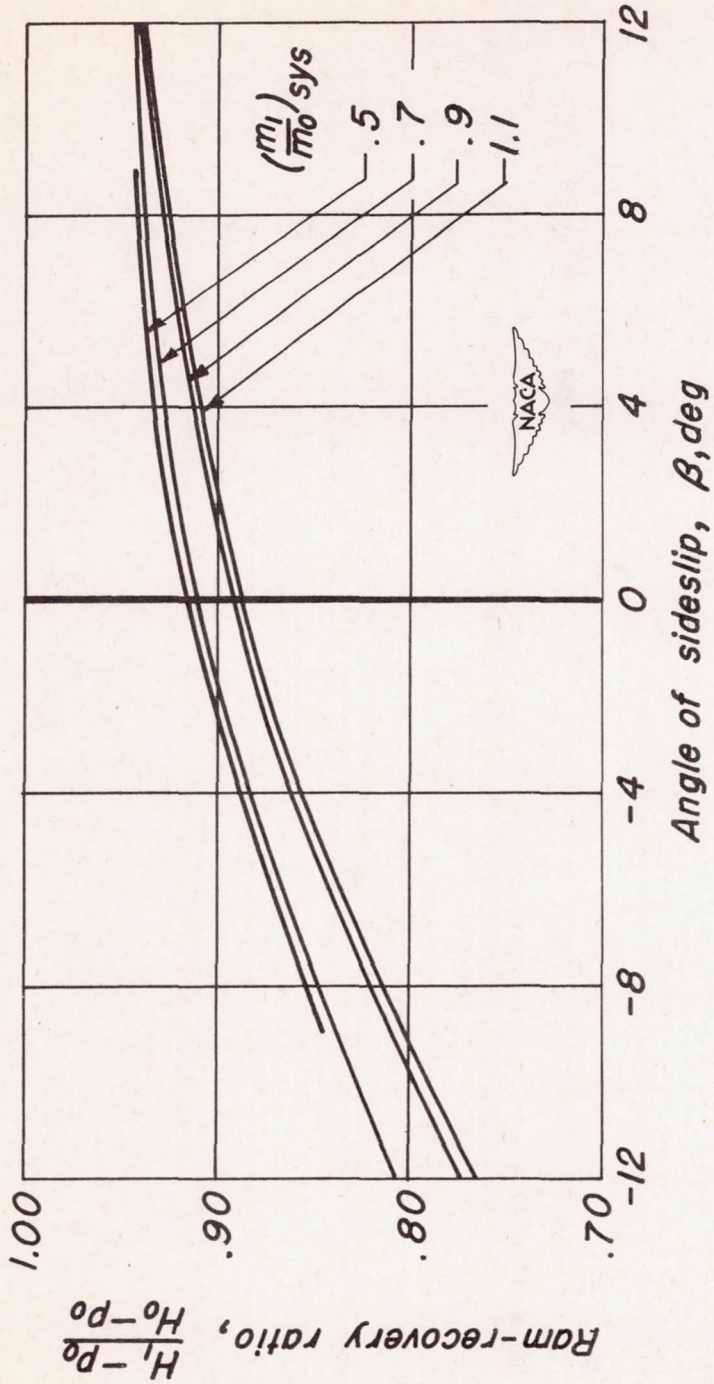

Figure 10.- The variation of entrance pressure recovery with sideslip of the right intake of a twin-intake installation; $\alpha = -2°$.

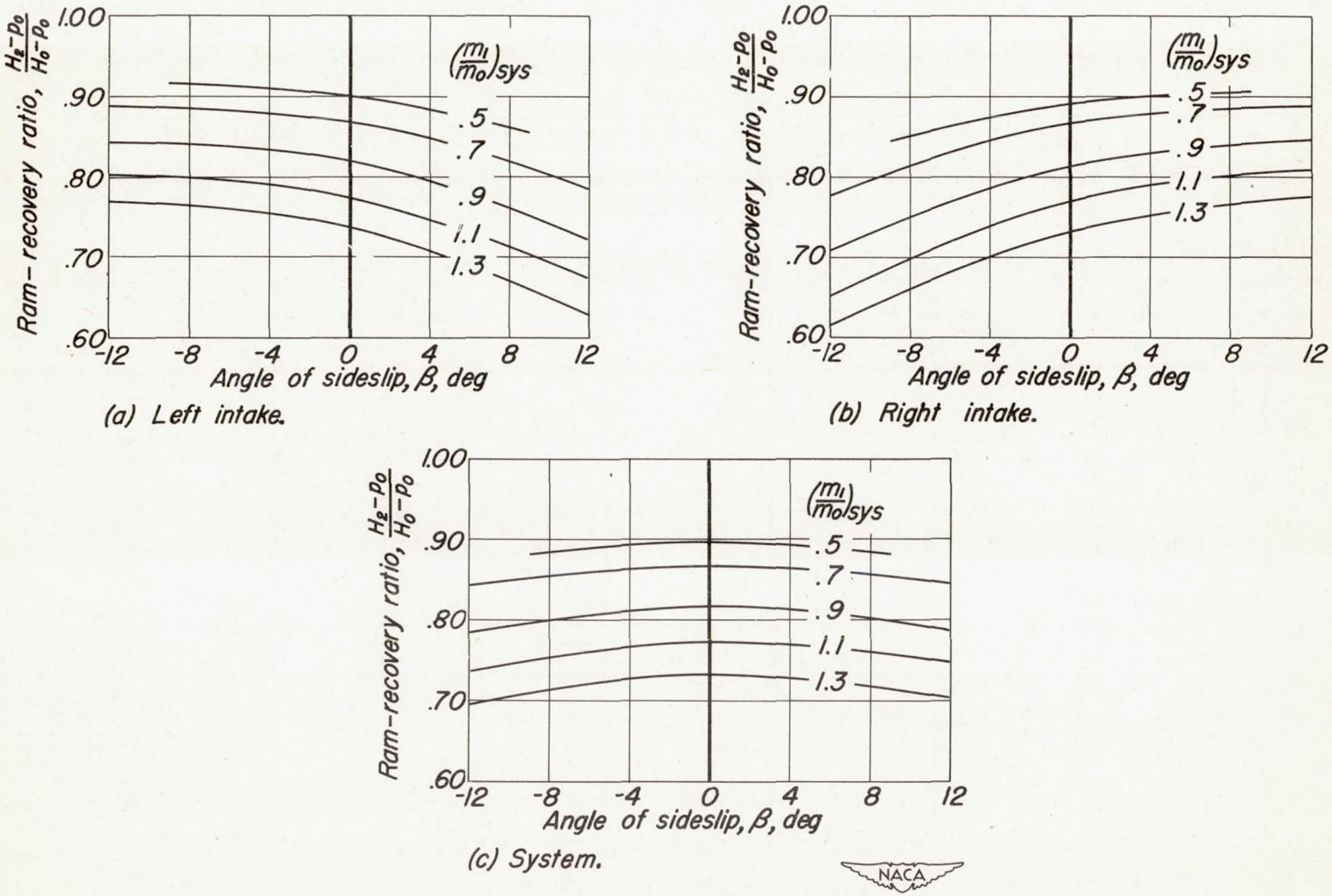

Figure 11.– The variation of pressure recovery, measured after partial diffusion, with sideslip of the twin-intake installation; $\alpha = -2°$.

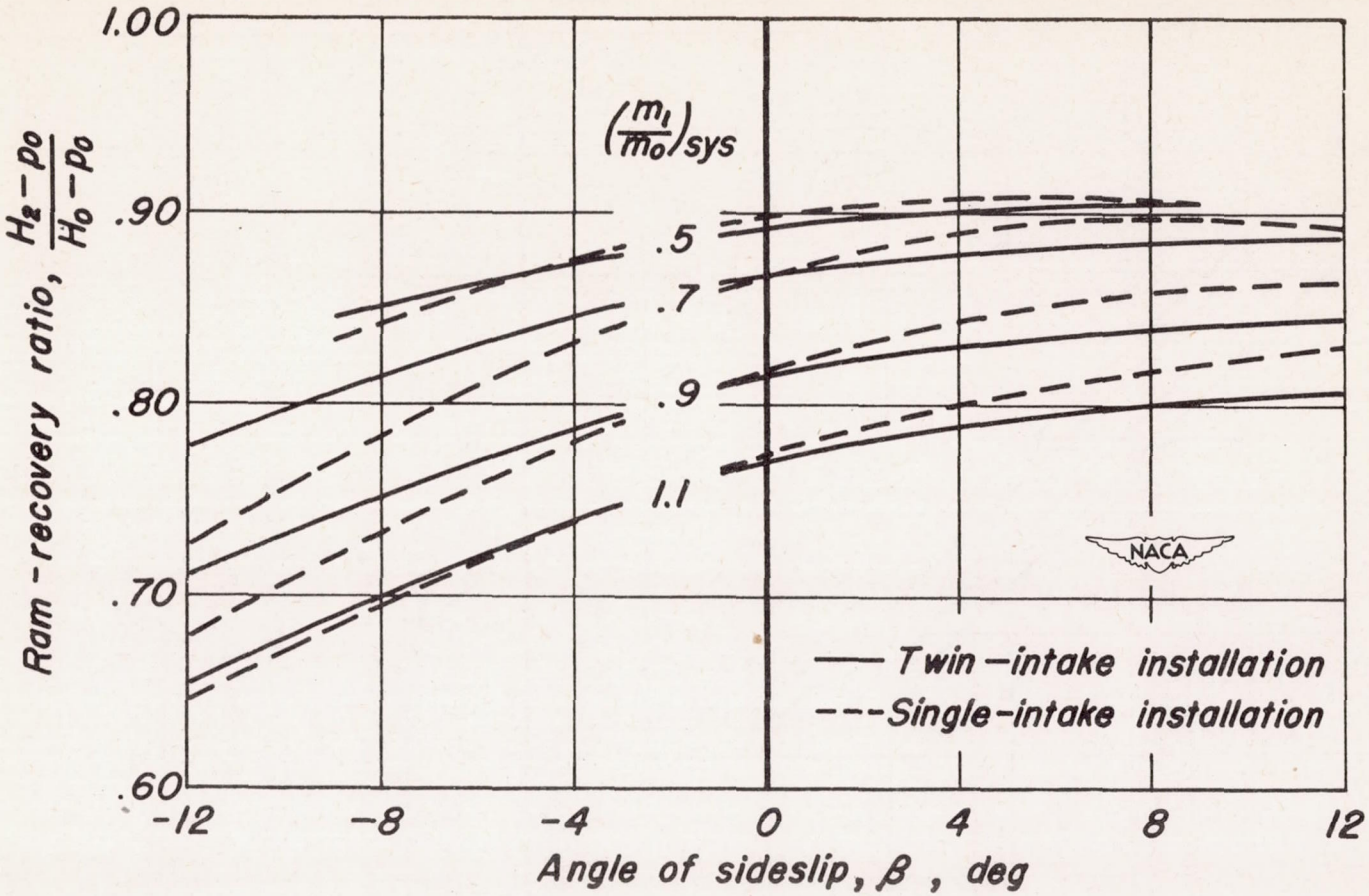

Figure 12. - A comparison of the pressure recovery, measured after partial diffusion, at various angles of sideslip of the right intake of a single-intake and a twin-intake installation; $\alpha = -2°$.

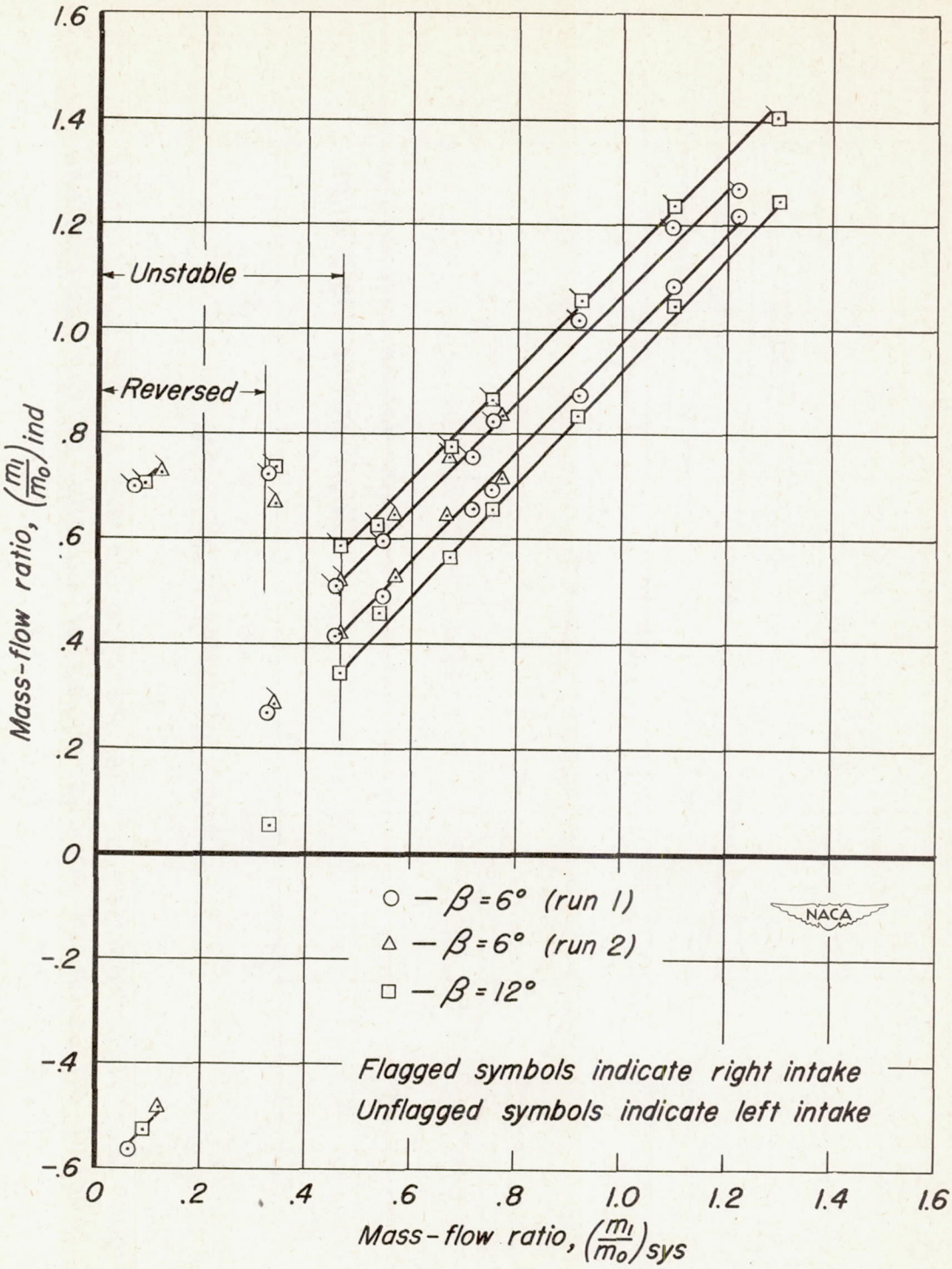

(a) $\beta = 6°, 12°$.

Figure 13.— The mass-flow ratio of each intake of a twin-intake installation as a function of the system mass-flow ratio; $\alpha = -2°$.

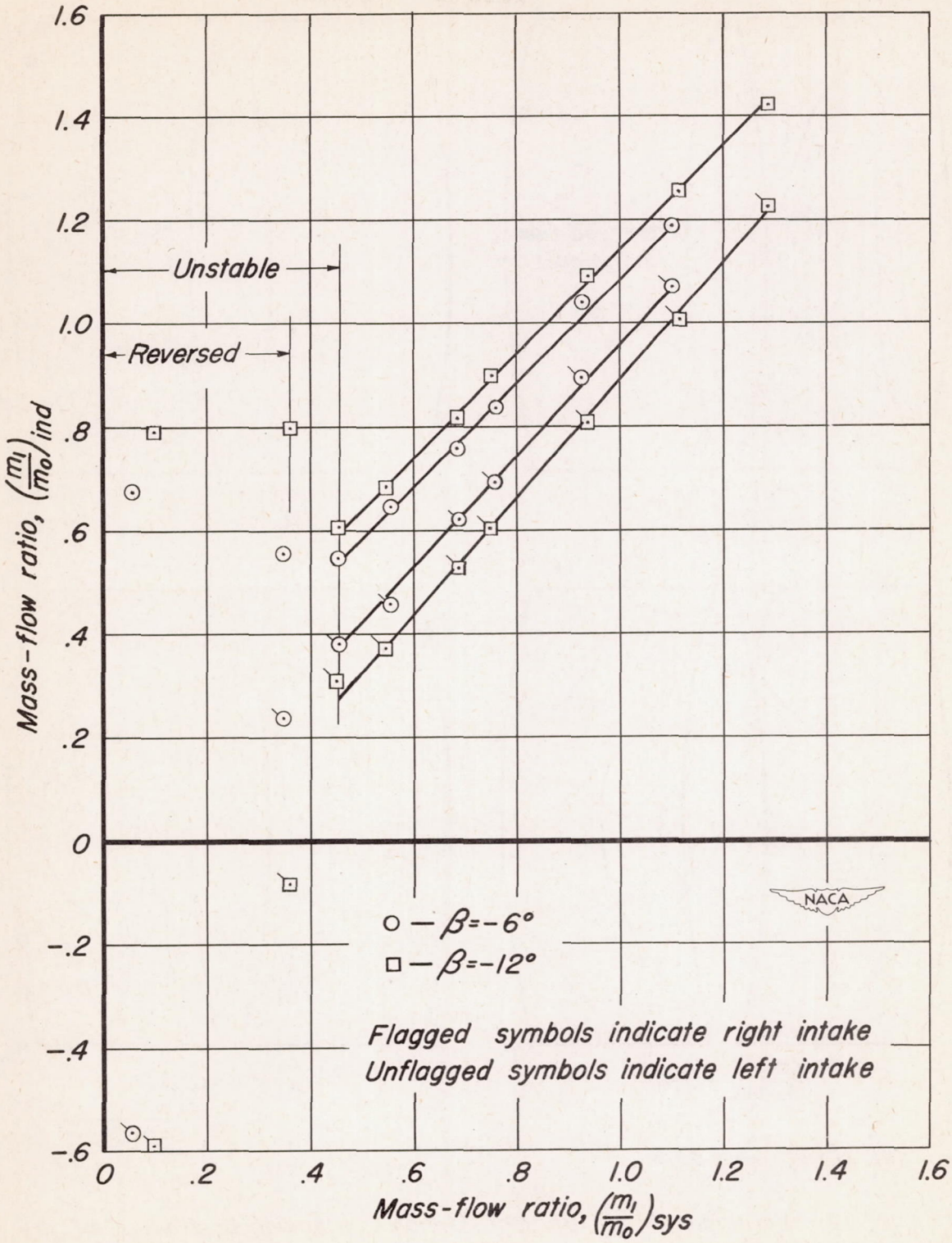

(b) β = -6°,-12°.

Figure 13.- Concluded.

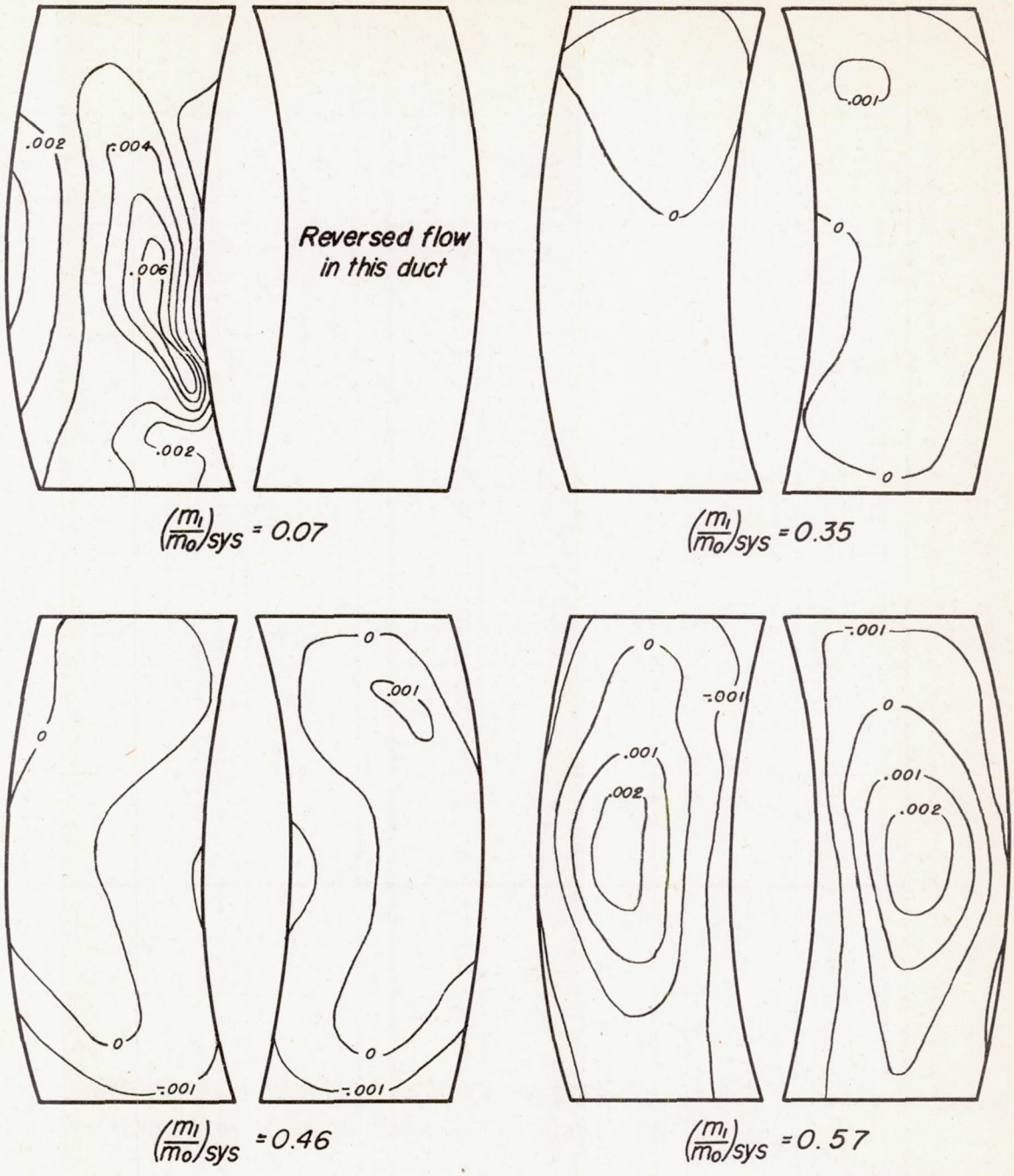

(a) $\beta = 0°$; $\frac{H_0}{q_0} = 33.8$.

Figure 14.– Variation of $\frac{\Delta H}{H_0}$ at duct station 2 (looking upstream) of the twin-intake installation; $\alpha = -2°$.

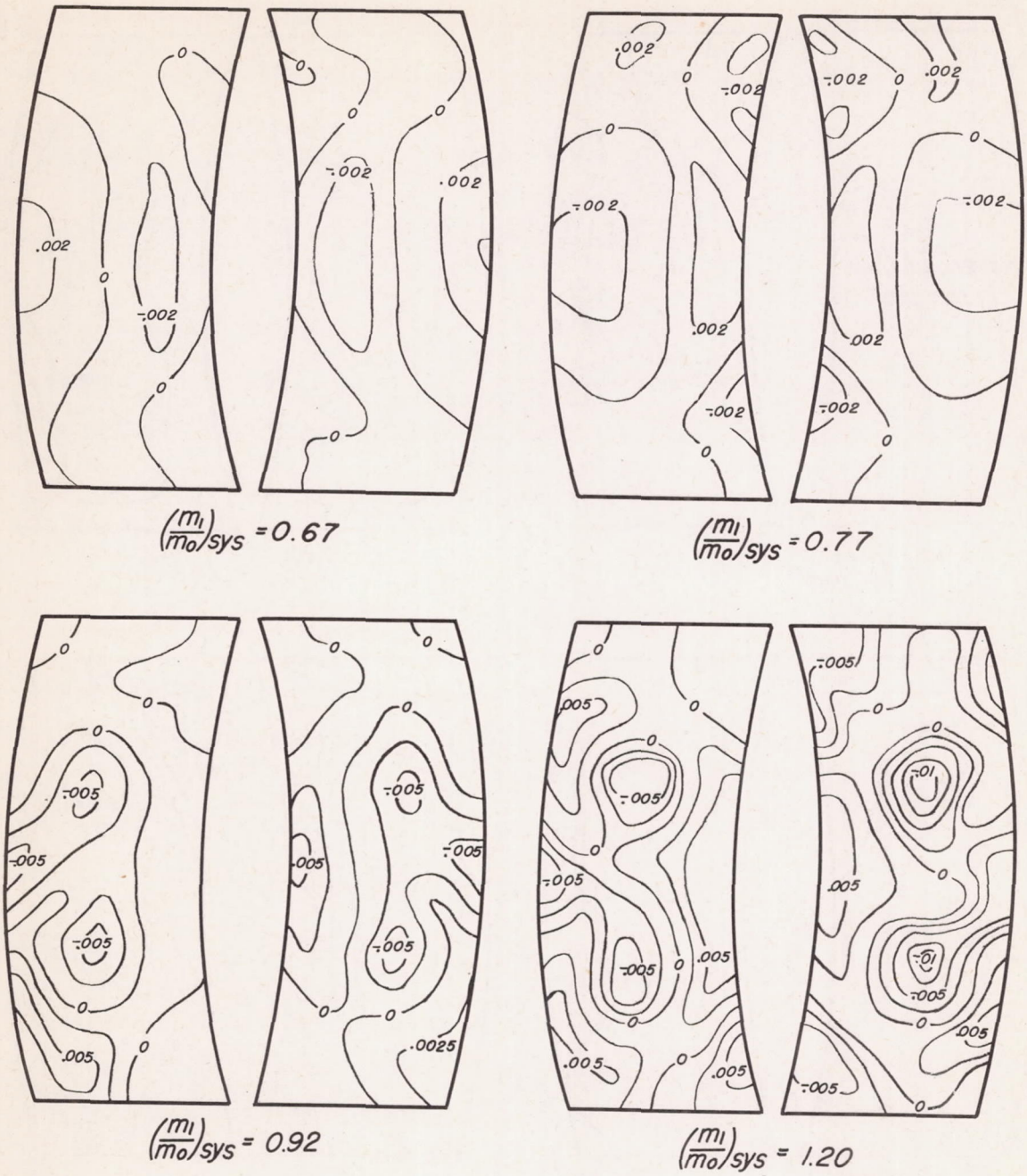

(b) $\beta = 0°$, $\frac{H_0}{q_0} = 33.8$.

Figure 14.– Continued.

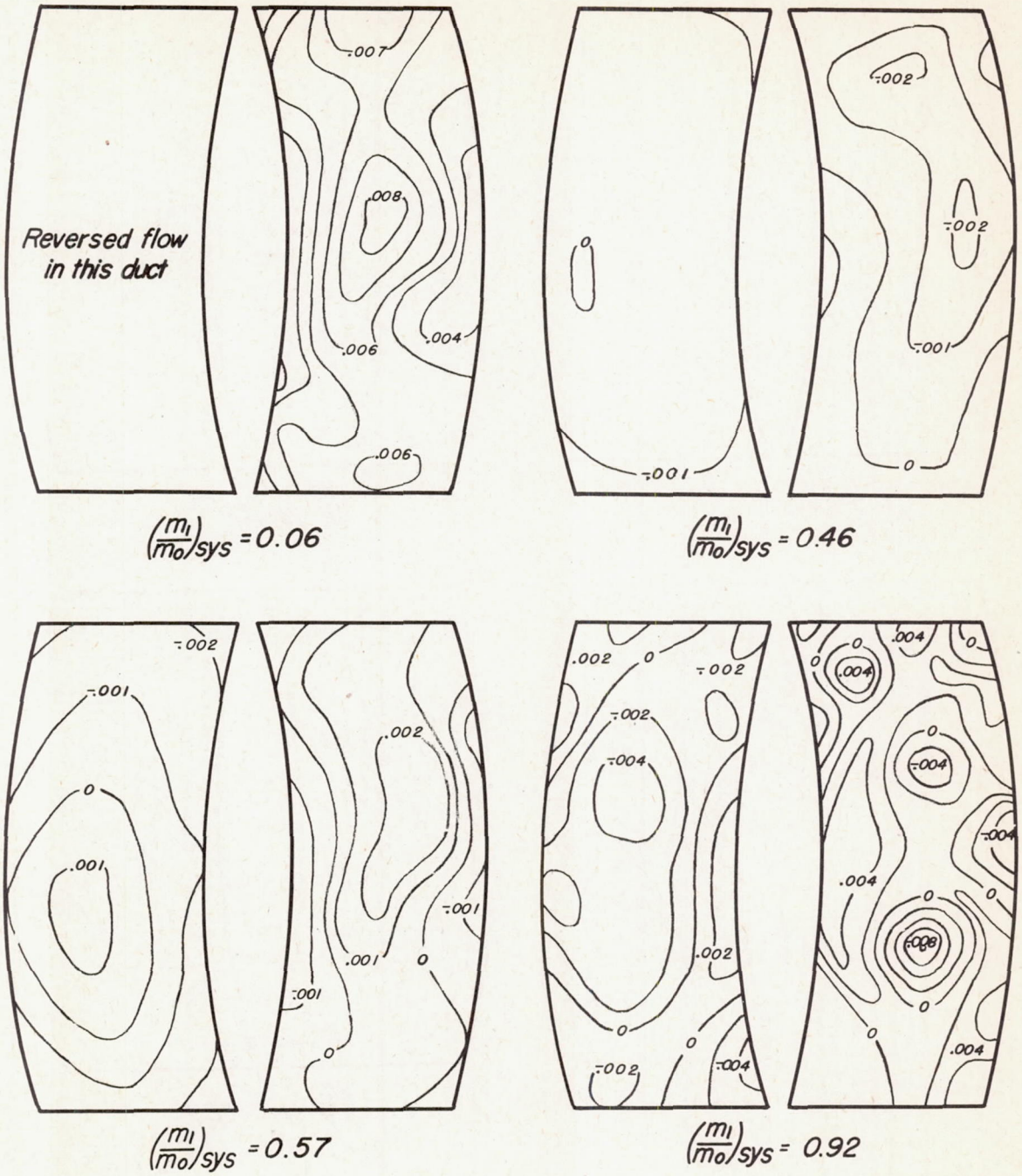

(c) $\beta = 6°$; $\frac{H_0}{q_0} = 33.8$.

Figure 14.- Continued.

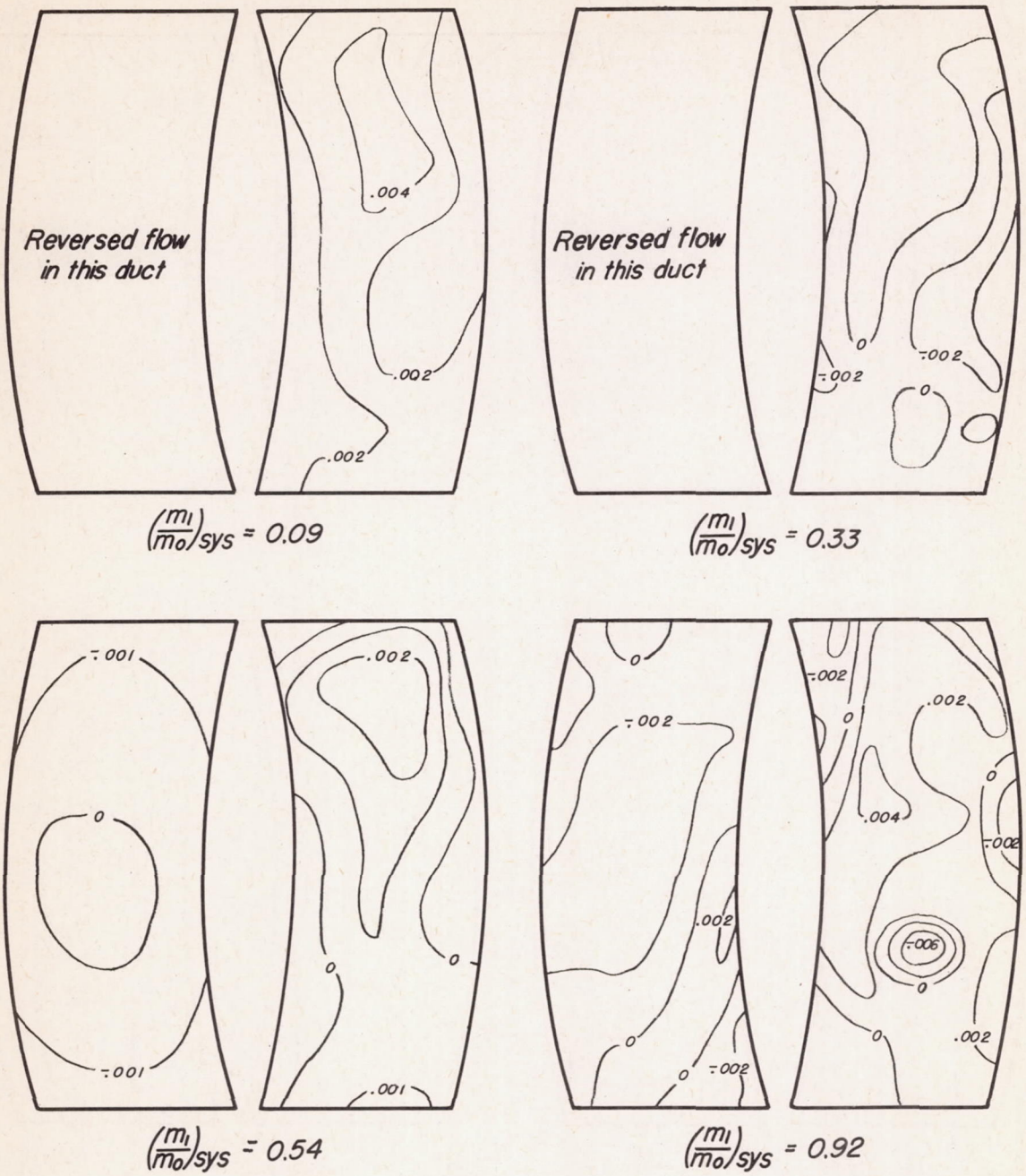

(d) $\beta = 12°$, $\frac{H_0}{q_0} = 54.4$.

Figure 14.- Concluded.

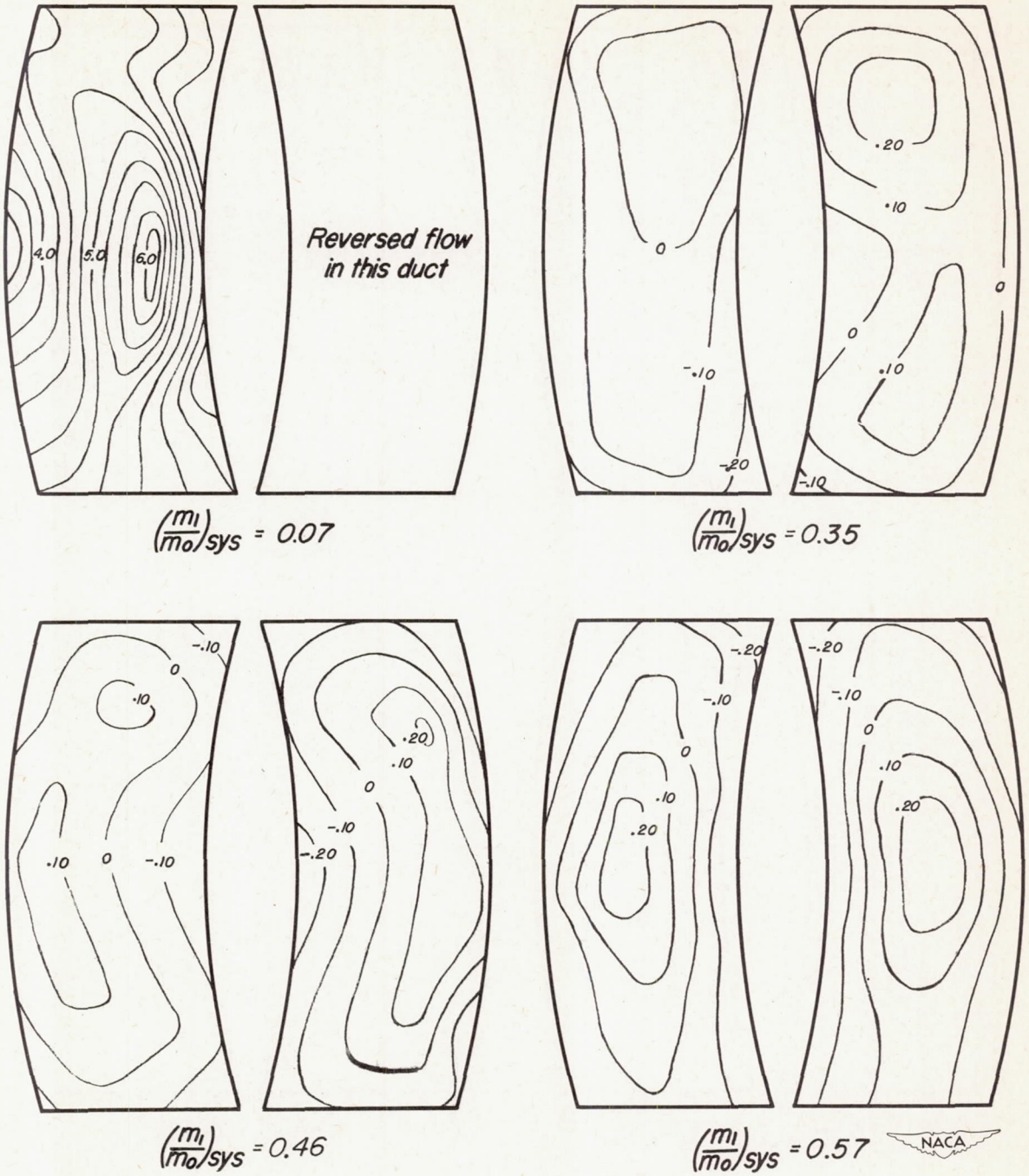

(a) $\beta = 0°$.

Figure 15.- Variation of $\left(\frac{V_l - V_{sys}}{V_{sys}}\right)$ at duct station 2 (looking upstream) of the twin-intake installation; $\alpha = -2°$.

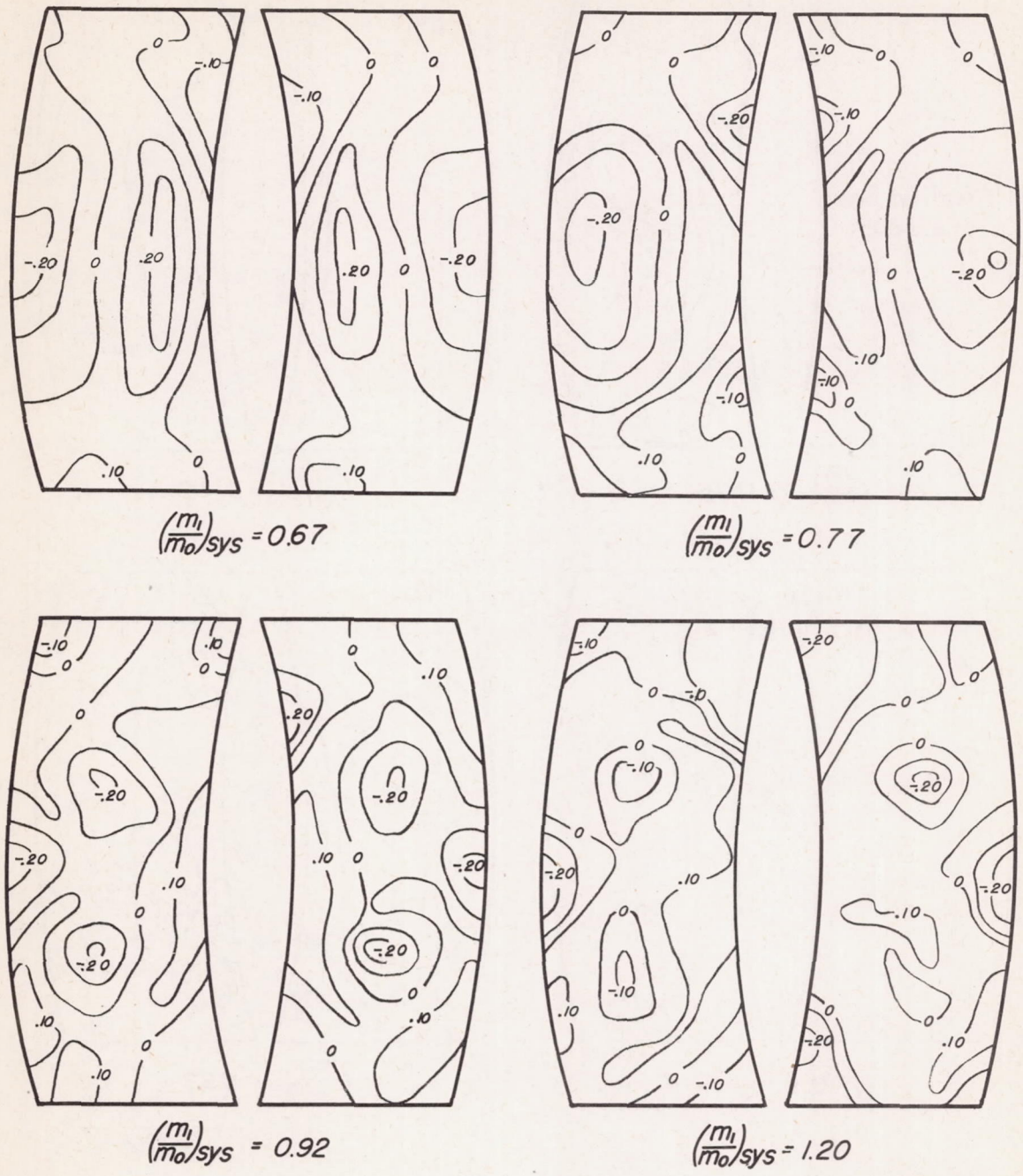

(b) $\beta = 0°$.

Figure 15.— Continued.

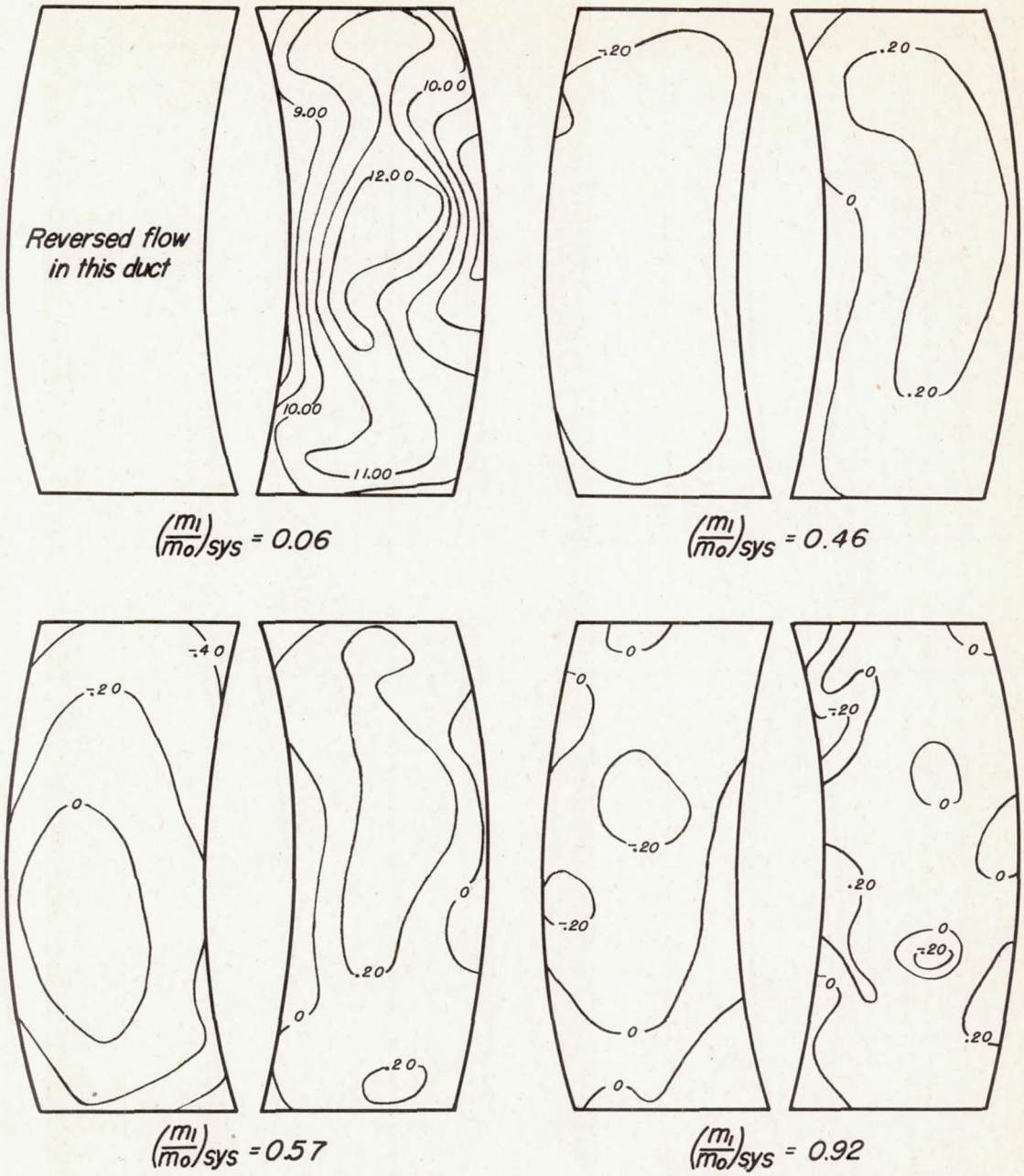

(c) $\beta = 6°$.

Figure 15.— Continued.

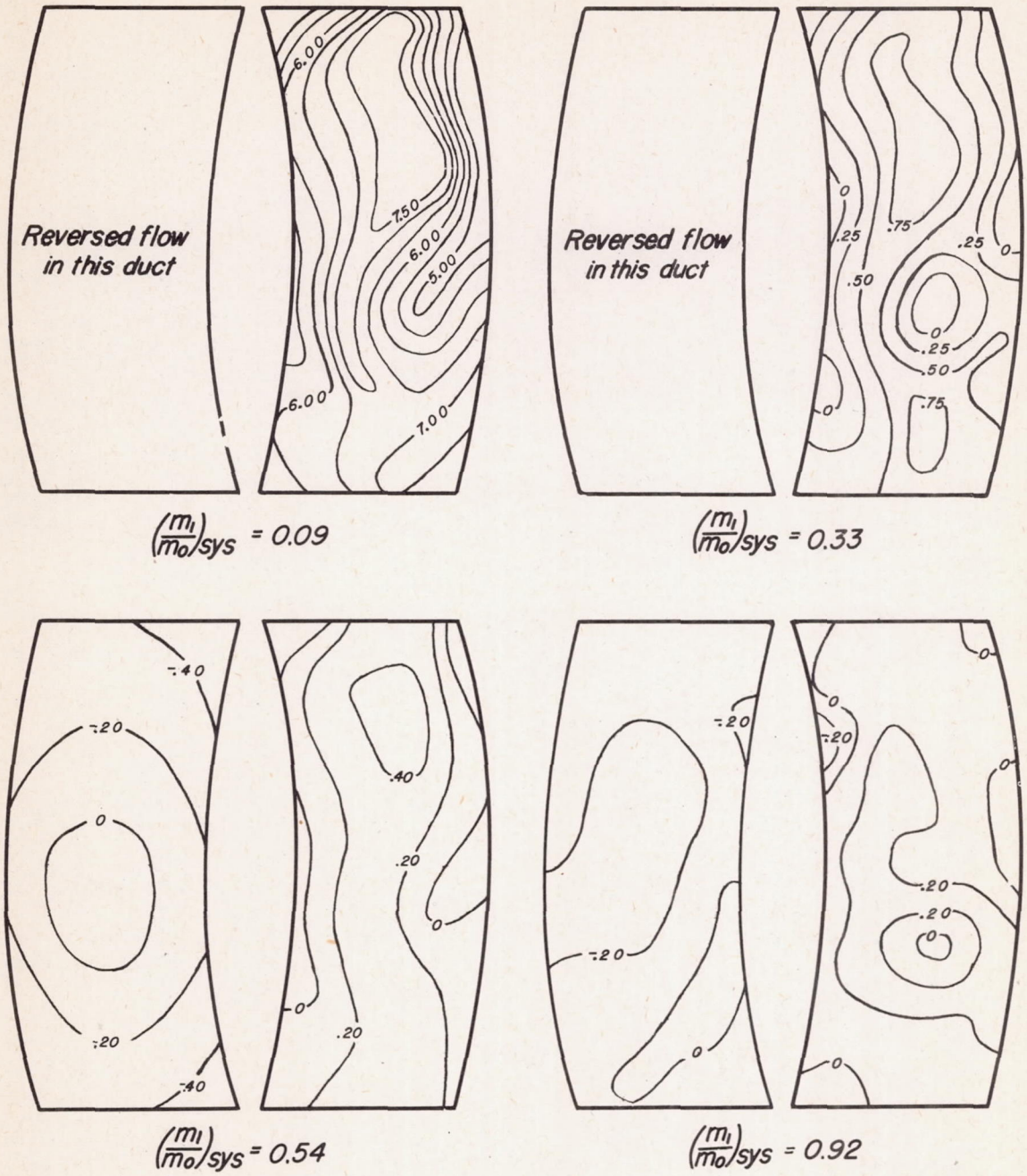

(d) $\beta = 12°$.

Figure 15.– Concluded.

NACA-Langley - 8-1-49 - 275